$1/f^{\alpha}$ density fluctuation at the slugging transition point of granular flows through a pipe

Akio Nakahara and Takeshi Isoda
Department of Physics, Chuo University, Kasuga, Bunkyo-ku, Tokyo 112, Japan
(Received 5 November 1996)

By changing the packing rate of metallic spheres inside a pipe, we experimentally investigated a density fluctuation of metallic spheres that fall through a vertical glass pipe filled with liquid. We found that only at the intermediate packing rate $p \sim 0.18$ the power spectrum of the density fluctuation of falling metallic spheres $P(f)$ obeys a power law as $P(f) \sim 1/f^{\alpha}$, where f is a frequency and α is a positive constant. This intermediate packing rate corresponds to a slugging transition point from the low-packing-rate region where metallic spheres fall almost freely to the high-packing-rate region where density waves (slugs of granular materials) emerge and so metallic spheres fall in a group very slowly. We also compare our experimental results with the jamming transition and the $1/f$ noise that appear in a crowded traffic flow. [S1063-651X(97)07604-6]

PACS number(s): 05.20.Dd, 83.70.Fn

I. INTRODUCTION

Due to its complex dynamic behaviors, the physics of granular materials has drawn the attention from scientists and engineers in various fields [1–3]. For example, flows of rough sand particles from a hopper produce nonuniform density waves [4]. However, experimental results [4] and also cellular-automata [5] and molecular-dynamics (MD) [6] simulations show that by using smooth sand particles no density waves are obtained. Therefore, the roughness of sand particles is the essence of the dynamics of the granular flow from the hopper. The power law for the power spectrum of the density fluctuation of falling sand particles has been obtained by the MD simulations [6].

Granular flows through a vertical pipe also produce density waves [7–9]. In the experiment, we pour rough sand particles into the hopper and let them fall down gravitationally from the hopper through a vertical glass pipe. Even if the granular flow from the hopper exit is set to be almost uniform and white-noise-like, the density waves of slugging sand particles emerge as the sand particles fall down through the vertical pipe.

MD simulations [7,10,11] and lattice-gas-automata (LGA) simulations [12,13] show that both the inelastic collision between rough sand particles and the friction due to the rough wall play important roles in the formation of density waves. On the other hand, in a previous paper [8] we reported that the hydrodynamic effect of fluid inside the pipe is not negligible. When the cock that is connected at the bottom of the vertical glass pipe is fully open, sand particles fall almost freely, even if we use rough sand particles. When the cock is closed to some extent, the back flow produced by the ascending air induces the formation of nonuniform granular flow, i.e., density waves [8]. To consider that this nonuniform granular flow is a kind of slug in a fluidized bed [14,15] in a narrow space, we can imagine the importance of the hydrodynamic effect due to the fluid filling the system [16]. We also found, in our previous paper [8], that the power-law power spectrum of the density fluctuation is self-organized only when the cock is properly half closed.

To exclude the roughness of granular materials and to emphasize the hydrodynamic effect of the fluid, we use, in this paper, smooth metallic spheres of almost equal sizes as granular materials. To investigate the hydrodynamic effect in more detail, we use water and the silicone oil with various kinematic viscosities and study how the granular flow changes as we vary the kinematic viscosity of liquid.

Now let us pay attention to a traffic flow problem. The relation between the density waves in granular flows and the traffic jams on crowded highways is pointed out [17]. In the traffic flow, vehicles move smoothly when the density of vehicles is low. As the density of vehicles increases, the system undergoes a dynamical jamming transition, and at a high-vehicle-density regime traffic jams appear and vehicles move in a group very slowly [17–24]. The power-law power spectrum was reported in the observation of real traffic flow [25], and numerical simulations showed that the power-law power spectrum appears only at a certain vehicle-density regime [26–30].

Considering that the vehicles correspond to falling granular materials through a pipe, we can expect that the slugging transition of granular flow and the jamming transition of traffic flow are similar phenomena. In fact, LGA simulations [12,13] show a slugging transition as the flow rate of granular materials is increased and the power-law power spectrum is observed only at a critical flow rate with the maximum transportation of granular materials. On the other hand, we can also imagine that the large kinematic viscosity of liquid prevents the growth of nonuniform granular flow since all granular materials fall very slowly when the kinematic viscosity of liquid is very large.

Thus the second aim of this paper is to check whether the slugging transition can be explained as a function of the packing rate of granular materials, just like the jamming transition in traffic flows. Since our first aim is to study the hydrodynamic effect on the formation of density waves, we have performed systematic experiments in which we control two dominant physical parameters, i.e., a packing rate of granular materials inside the pipe and a kinematic viscosity of the liquid that fills the pipe. We investigated the behavior of the granular flow and its power spectrum in each experimental condition.

In the following sections we show that in the high-Reynolds-number condition the slugging transition is ex-

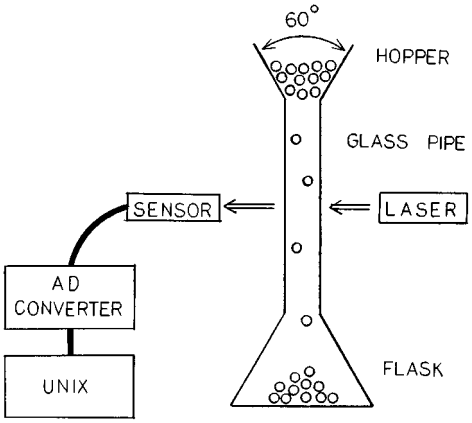

FIG. 1. Schematic illustration of the experimental setup. The whole system is filled with liquid. Metallic spheres are put onto the hopper and fall from the hopper gravitationally through a vertical pipe. To measure the granular flow, a set of a semiconductor laser and a photodetecting sensor is placed horizontally across the vertical glass pipe. The output signal of the photodetecting sensor is transferred through an analog-to-digital (AD) converter to a UNIX system (SPARC Station 2, SunMicrosystems), where the FFT analysis is performed to obtain the power spectrum of the density fluctuation.

pressed by the jamming transition, while in the low-Reynolds-number condition the high kinematic viscosity of liquid prevents the growth of nonuniform granular flows. We show also that we can obtain the power law for the power spectrum only at the slugging transition point.

This paper is organized as follows. In Sec. II we explain the methods of our experiments. In Secs. III, IV, and V we present our experimental results. First, in Sec. III we show how the granular flow changes by varying the packing rate of metallic spheres inside the pipe. In our experiments, the nonuniform granular flow is self-organized as granular materials fall down from the hopper through a vertical pipe. In Sec. IV we present the results of our study about the self-organization of the density fluctuation, performed by changing the measuring position from the hopper to the pipe end. In Sec. V we explain our experiments in which we use silicone oil with various kinematic viscosities. We summarize our results in Sec. VI.

II. METHODS OF EXPERIMENTS

The experimental setup is described schematically in Fig. 1. As granular materials we use smooth metallic spheres of almost equal sizes, such as lead spheres and stainless-steel spheres. We set a hopper at the top of a vertical glass pipe and insert the pipe end into a flask.

To observe the flow of granular materials, we use a charge coupled device camera and a videorecording system. We also place a set of a semiconductor laser and a photodetecting sensor (LX2-02, Keyence Co., Japan) horizontally at both sides of the vertical pipe and check the time evolution of the intensity of the transmitted light across the vertical pipe. Here the wavelength of the laser is 780 nm. The beam of the laser consists of a bundle of straight beams, and the cross section of the laser beam and the size of the window of the photodetecting sensor are both 1.0 mm in height and 10.0 mm in width. Since the inner diameter of the vertical pipe is less than the width of both the laser beam and the window of the sensor in our experiments, we obtain the data that are averaged across the horizontal direction, i.e., we obtain the data of the one-dimensional granular flow along the vertical pipe.

In our experiments we use three kinds of metallic spheres, i.e., lead spheres 1.04 ± 0.10 mm($\sim$1.0 mm) and 1.68 ± 0.08 mm($\sim$1.7 mm) in diameter and stainless-steel spheres 1.637 ± 0.003 mm($\sim$1.6 mm) in diameter. As the liquid we use water and silicone oil with various viscosities. The density of silicone oil with any viscosity is the same as that of water and is given by 1.0 g/cm^3. The kinematic viscosity ν of water is 1.0 mm^2/s and that of silicone oil is varied as 0.65, 1.00, 2.00, 3.00, 3.24, 3.50, 4.00, 5.00, 10.0, 20.0, and 50.0 mm^2/s.

We use two kinds of glass pipes, i.e., 7.0 and 9.0 mm in inner diameter. Since the diameters of metallic spheres we use are varied from 1.0 to 1.7 mm, the value of the aspect ratio of the inner diameter of the glass pipe to the diameter of metallic spheres is smaller than 10 in any case. When the value of this aspect ratio is greater than 10, the system does not show any characteristic features of the nonuniform granular flow, i.e., granular materials do not produce the density fluctuation.

As for the length of the pipe, we cannot see any difference in our experimental results by changing it from 700 to 1500 mm. That is, the 700-mm-length pipe is enough for our experiments because, as will be shown later, the granular flow through the pipe self-organizes into a stationary structure before granular materials fall 200 mm down from the hopper.

To change the packing rate of metallic spheres inside the pipe, we use an additional hopper and put it onto the original hopper, which is directly connected to the glass pipe. The opening angle of the original hopper and that of an additional hopper are the same. Here the inner diameters of both the glass pipe and the original hopper are exactly the same, but that of the additional hopper is a bit smaller. Thus we can decrease only the input rate of granular materials by this setup. By changing the inner diameter of the additional hopper, we can control the input rate of metallic spheres into the glass pipe.

To change the input rate systematically, we use the additional hopper alternatively with slightly different inner diameters. Then we calculate the value of the packing rate p for each additional hopper by the relation

$$p=\frac{M}{v_g TS}. \tag{1}$$

Here S is the cross section of the pipe $S=\pi r^2$, where r is an inner radius of the pipe; M is the total volume of metallic spheres we use in our experiments; T is the total time needed for all these metallic spheres to fall from the hopper and thus M/T is the input rate of metallic spheres from the hopper into the pipe; and v_g is the mean velocity of falling granular materials (metallic spheres) and is given by $v_g=1/2L$ m/s, where L is the mean time needed for metallic spheres to fall down 50 cm vertically through the pipe. We measure values of T and L experimentally for each additional hopper and obtain the value of p.

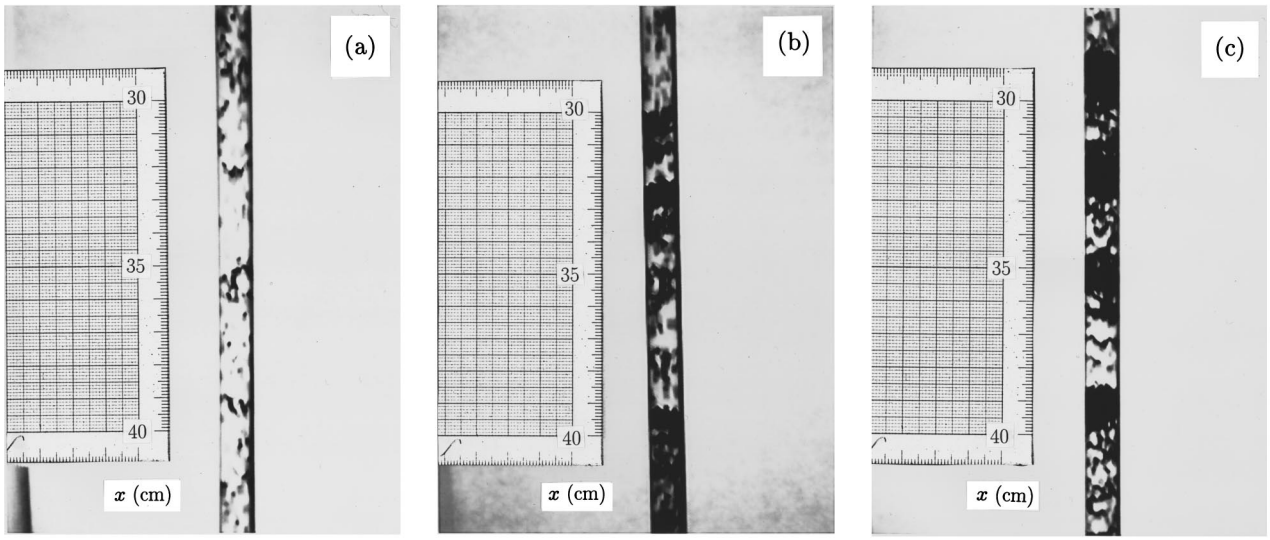

FIG. 2. Snapshots of the granular flow through a vertical glass pipe, where the packing rate is $p=0.05$, 0.18, and 0.21 in (a), (b), and (c), respectively. Here we used lead spheres 1.7 mm in diameter, a glass pipe 9.0 mm in inner diameter, and water as the liquid. All metallic spheres fall downward gravitationally. The measure is vertically set at the left-hand side of the vertical glass pipe from $x=30$ to 40 cm, where x is a vertical distance down from the hopper.

Since we are interested in the flow of granular materials in the pipe, we should check whether or not this additional hopper itself produces the density fluctuation. We performed the fast Fourier transform (FFT) analysis directly to the granular flow at the hopper exit and confirmed that the granular flow from the additional hopper is almost uniform and white-noise-like. This means that the additional hopper only changes the input rate of metallic spheres, but it does not produce the density fluctuation at the hopper exit. The density fluctuation is self-organized as metallic spheres fall down through the pipe.

III. DEPENDENCE ON THE PACKING RATE

Now we will present our experimental results. Figures 2–5 have been obtained from our experiments in which we used water as the liquid, lead spheres 1.7 mm in diameter as metallic spheres, and a glass pipe 9 mm in inner diameter and 700 mm in length. Note that the free fall velocity v_0 of a single lead sphere 1.7 mm in diameter is experimentally given by $v_0=0.62$ m/s in water and its Reynolds number Re $= dv_0/\nu$ is Re $= 1054$. The total mass of lead spheres used in our experiments is 2 kg. Since the density of lead is 11.34 g/cm^3, the total volume of lead spheres is $M=176$ cm^3.

The packing rate we get without the additional hopper is 0.36 in this case. By using additional hoppers, we can vary the packing rate as 0.36, 0.30, 0.26, 0.21, 0.18, 0.16, 0.14, 0.11, 0.09, and 0.05.

First, Fig. 2 shows snapshots of the density fluctuation of granular flows at $x=40$ cm as functions of the packing rate p. Here x is defined as a distance down from the hopper and indicates the position where we take data. Packing rates p are given by $p=0.05$ in Fig. 2(a), $p=0.18$ in Fig. 2(b), and $p=0.21$ in Fig. 2(c), respectively. In Fig. 2(a) with $p=0.05$, we see only a faint density fluctuation, while in Fig. 2(c) with $p=0.21$ we can clearly observe slugs of metallic spheres, i.e., density waves. That is, in the low-packing-rate region metallic spheres fall almost freely as shown in Fig. 2(a), but in the high-packing-rate region [see Fig. 2(c)] metallic spheres form slugs and fall in a group very slowly. This is a dynamical transition from a free-fall region to a slugging region. Figure 2(b) with $p=0.18$ corresponds to the pattern at the intermediate-packing-rate region, i.e., the slugging transition point from the low-packing-rate free-fall region to the high-packing-rate slugging region.

In Fig. 3 we see a time evolution of the transmitted light intensity at $x=40$ cm, measured by our photodetecting sen-

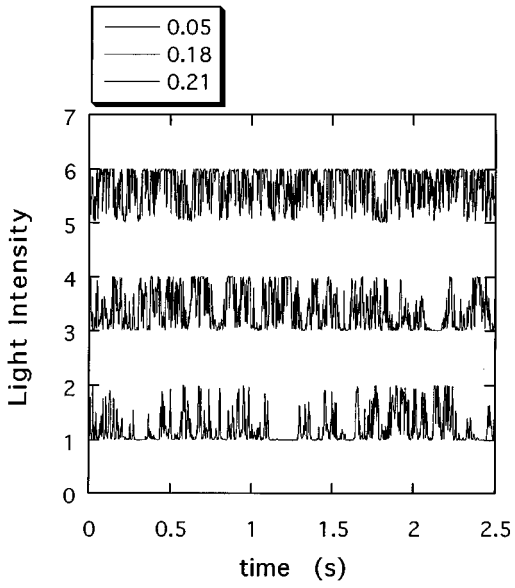

FIG. 3. Time evolution of the transmitted light intensity as a function of time t at $x=40$ cm with various packing rates p. Here we used lead spheres 1.7 mm in diameter, a glass pipe 9.0 mm in inner diameter, and water as the liquid. The values of the packing rate p are, from top to bottom, 0.05, 0.18, and 0.21, respectively. These solid lines are shifted vertically one by one.

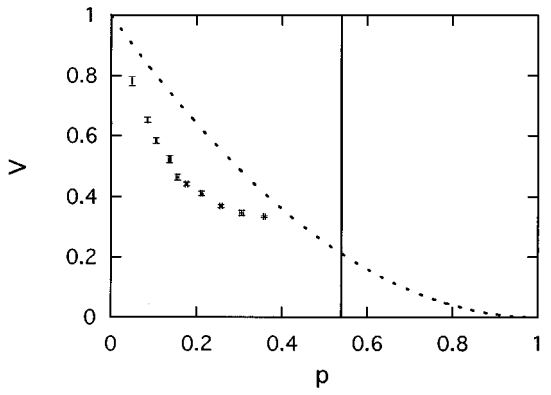

FIG. 4. Normalized relative velocity between falling metallic spheres and ascending fluid V plotted as a function of the packing rate p. Here we used lead spheres 1.7 mm in diameter, a glass pipe 9.0 mm in inner diameter, and water as the liquid. The vertical solid guide line represents the maximum packing rate $p_m=0.54$ for this case. The dotted guide line denotes V of the gravity-dominated flow in an infinite system and is given by $V=(1-p)^2$.

sor. Here the light intensity is normalized to unity. That is, when the value of the transmitted light intensity is unity, this means that there are no metallic spheres in front of the photodetecting sensor at that time. As the number of metallic spheres that cross the sensor increases, the value of the transmitted light intensity decreases and at zero intensity no light can transmit across the pipe. Thus the high intensity corresponds to the low granular density and vice versa. The time evolution of the transmitted light intensity when $p=0.05$ resembles a white-noise pattern, while that for $p=0.21$ shows a complex pattern with many flat regions with zero intensity. Here the zero intensity regions correspond to slugs of metallic spheres.

As described above, the free-fall velocity v_0 of a single lead sphere 1.7 mm in diameter is $v_0=0.62$ m/s in water. Since the glass pipe is directly connected to the flask and therefore liquid cannot go outside of our closed system, we obtain the conservation relation

$$pv_g+(1-p)v_f=0. \tag{2}$$

Here p is a mean packing rate of granular materials inside the pipe and thus $1-p$ is that of liquid; $v_g\geqslant 0$ is the mean velocity of granular materials (metallic spheres) and $v_f\leqslant 0$ is that of fluid (liquid), respectively. We set the direction of the gravity as positive. Since we can obtain values of v_g and p by the method described above, Eq. (2) gives us the value of v_f. The conservation relation (2) means that, as granular materials fall down through the pipe, the liquid should go up due to the excluded volume effect, i.e., the incompressibility of liquid. Therefore, we introduce a normalized relative velocity V between falling metallic spheres and ascending liquid, which is defined as

$$V=\frac{v_g-v_f}{v_0}\geqslant 0. \tag{3}$$

In Fig. 4 the normalized relative velocity V is plotted with error bars as a function of the packing rate p. The solid vertical guide line represents the maximum packing rate p_m for the case where lead spheres 1.7 mm in diameter fill the glass pipe 9 mm in inner diameter and its experimental value is given by $p_m=0.54$. The dotted guide line denotes V of the gravity-dominated flow in an infinite wallless system and is given by $V=(1-p)^2$ [31]. Note that the experimental value of V in the pipe flow is always smaller than $V=(1-p)^2$. In the narrow pipe, metallic spheres cannot move as freely as those falling in the infinite system because the finite-size effect as well as the friction by the wall induces the growth of the density fluctuation and thus helps the formation of slugs.

In the low-packing-rate region ($p<0.18$), as seen in Fig. 4, the value of V decreases rapidly as the value of p increases. This is because, even though almost all metallic spheres fall freely in this region, those few metallic spheres that form a density fluctuation reduce the mean velocity V as a whole [see Fig. 2(a)]. In the high-packing-rate region ($p>0.18$) most of the metallic spheres are trapped in slugs, as shown in Fig. 2(c), and V is relatively low. The intermediate packing rate ($p\sim 0.18$) is a slugging transition point from the low- to the high-packing-rate region. That is, at this intermediate packing rate some metallic spheres are trapped in slugs while some others fall freely.

This change from the low-packing-rate free-fall region to the high-packing-rate slugging region is not a sharp and clear phase transition as long as we use a liquid as the fluid. That is, it is rather a continuous crossover from one state to the other. As for the slugging transition of sand particles in the air, however, this change is a sharp and clear phase transition. This difference between these two cases can be attributed to the role of fluid (i.e., liquid or gas) in the formation of slugs and is still under investigation. As will be shown below, at this intermediate packing rate ($p\sim 0.18$) the behavior of the power spectrum of the density fluctuation changes drastically. The power-law power spectrum is obtained at this intermediate packing rate only.

Next we present our experimental results on the power spectra of the density fluctuation of falling metallic spheres, performed by changing the packing rate p. Figure 5 shows the power spectra of the density fluctuations at $x=40$ cm as the functions of the frequency f at the various packing rates. Here the values of p are, from top to bottom, 0.05, 0.09, 0.11, 0.14, 0.16, 0.18, 0.21, 0.26, 0.30, and 0.36. The vertical scale for each spectrum is shifted appropriately. Note that each power spectrum has a sharp edge at about $f\sim 100$ Hz. Since the mean velocity of the falling metallic spheres is about 0.2 m/s and the height (vertical size) of the window of the photodetecting sensor is 1 mm, the mean time needed for one metallic sphere to cross the sensor vertically is about 0.005 s. For our system, twice this time (i.e., 0.01 s) is the resolving power of the photodetecting sensor, so our system cannot measure high-frequency variation for $f>100$ Hz. That is the reason why all our power spectra have sharp edges. (The precise value of the edge depends also on the value of V for each p.)

We also note, from the time evolution of the transmitted light intensity (see Fig. 3), that the time needed for one slug to cross the photodetecting sensor vertically is greater than about 0.15 s, which corresponds to a frequency of $f<3$ Hz. From this order estimate, we can classify the frequency region into two ranges, i.e., the high-frequency range (3 Hz

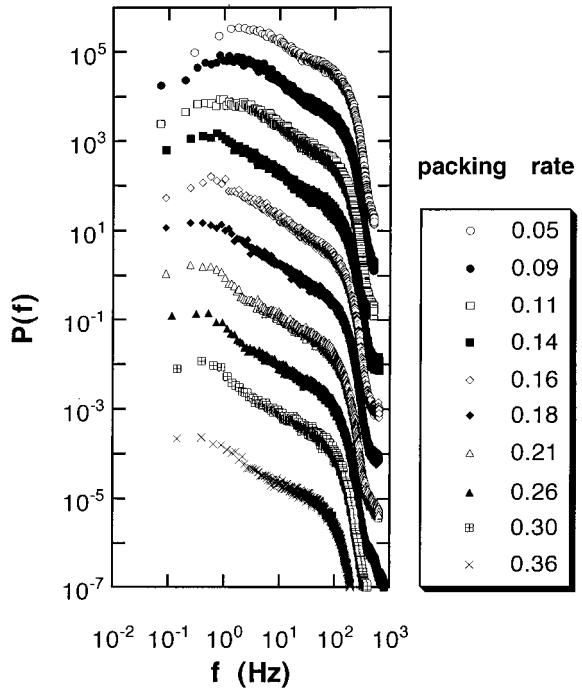

FIG. 5. Power spectra of the density fluctuation as functions of the frequency f at $x=40$ cm with various packing rates p. Here we used lead spheres 1.7 mm in diameter, a glass pipe 9.0 mm in inner diameter, and water as the liquid. From top to bottom, the packing rates p of lead spheres are 0.05, 0.09, 0.11, 0.14, 0.16, 0.18, 0.21, 0.26, 0.30, and 0.36. The vertical scale for each spectrum is shifted appropriately. The spectrum at each p was obtained by averaging over ten trials.

$<f<$ 100 Hz), where the power spectra describe the microscopic density fluctuation of metallic spheres, and the low-frequency range ($f<3$ Hz), where the power spectra describe the macroscopic movements of slugs, i.e., density waves.

At low packing rates such as $p=0.05$, 0.09, and 0.11, the power spectra do not show definite tendencies and are white-noise-like in the low-frequency range. This feature means that most metallic spheres fall freely and randomly and only few clusters are observed macroscopically. On the other hand, at high packing rates such as $p=0.21$, 0.26, 0.30, and 0.36, power spectra are monotonically decreasing functions of p and the values of power spectra in the low-frequency range become relatively high, which means that there are many slow clusters that form slugs. Furthermore, at the intermediate packing rate $p=0.18$, the power spectrum obeys the power law as $P(f)\sim 1/f^{\alpha}$, where α is a positive constant given as $\alpha=0.81\pm 0.01$ over a wide frequency range of 0.5–50 Hz.

The value $\alpha\simeq 0.81$ is smaller than the value $\alpha\simeq 1.5$ obtained in our previous experiments on the rough sand particles in air [8]. We consider that this difference is due to the hydrodynamic effect of fluid (liquid or gas) on the formation of slugs and is still under investigation.

To summarize this section, in Fig. 6 we show a schematic illustration of the changes of power spectra as we increase the packing rate p. At the low packing rate most metallic spheres fall freely and we can observe only a faint density fluctuation macroscopically. Therefore, the power spectrum

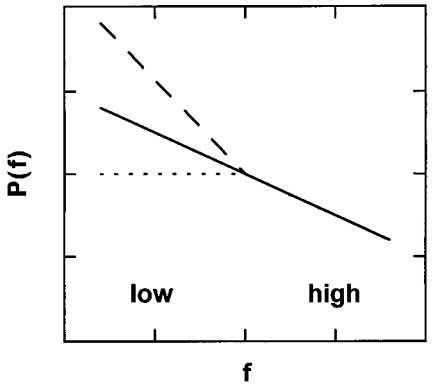

FIG. 6. Schematic illustration of the changes of power spectra $P(f)$. The dotted line denotes the power spectrum in the low-packing-rate free-fall region, the solid line denotes that for the intermediate packing rate, and the dashed line denotes that in the high-packing-rate slugging region. Only at the intermediate packing rate (i.e., at the slugging transition point), the power spectrum shows a single-power-law behavior $P(f)\sim 1/f^{\alpha}$ over a wide frequency range, i.e., in both the low- and the high-frequency ranges.

in the low-frequency range shows a white-noise-like behavior, as shown by the dotted line in Fig. 6. As the packing rate increases, the amplitude of the power spectrum at the low-frequency range increases. This suggests the growth of the macroscopic structure in the granular flow. At the intermediate packing rate (i.e., at the slugging transition point), slugs begin to emerge and the time evolution of the transmitted light intensity, shown in Fig. 3, looks almost scale invariant. This almost-scale-invariant feature suggests that the granular flow has a complex spatiotemporal structure without any characteristic length scale or any characteristic time scale.

As we increase the packing rate, the amplitude of the power spectrum at the low-frequency range increases and, as shown by the dashed line in Fig. 6, the power spectrum no longer obeys a single power law. This is because once stable slugs are formed in the high-packing-rate slugging region, the system acquires a macroscopically stationary slugging structure with some characteristic length and time scales. The granular flow no longer shows a scale-invariant behavior. These are our experimental results as for the dependence of power spectra on the packing rate.

IV. SELF-ORGANIZATION

Now let us explain our experiments on the self-organization of a nonuniform granular flow through a pipe. Since the density fluctuation of falling metallic spheres is produced as metallic spheres fall down from the hopper through a pipe, we study the formation of the density fluctuation by changing the measuring position from the hopper to the pipe end. As described above, the hopper flow, i.e., the granular flow at the hopper exit, is of a white noise, so the density fluctuation is self-organized through a pipe [8,32]. The values of physical parameters used in this section are exactly the same as those described in Sec. III.

First, we present experimental results as for the high-packing-rate slugging region. Figure 7 shows the time evolution of the transmitted light intensity at various x for $p=0.21$. Figure 8 represents power spectra as functions of

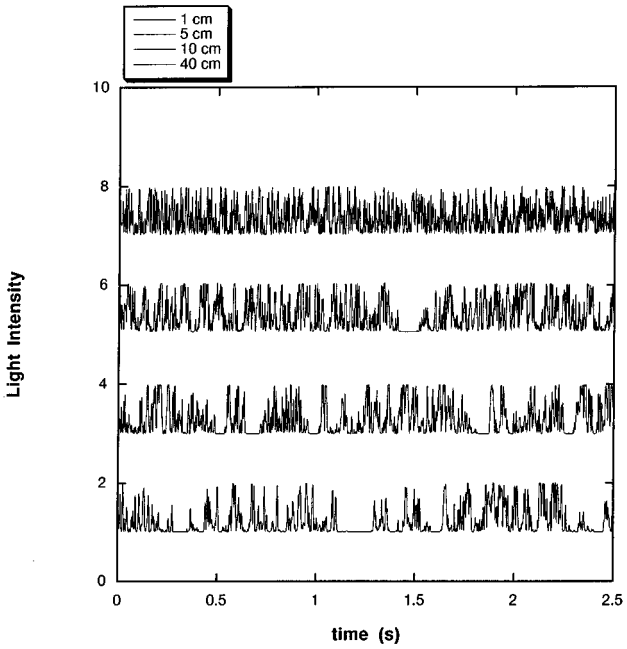

FIG. 7. Time evolution of the transmitted light intensity as a function of time t for $p=0.21$ at various measuring positions x, where x is the distance between the hopper exit and the measuring position. Here we used lead spheres 1.7 mm in diameter, a glass pipe 9.0 mm in inner diameter, and water as the liquid. The value of x is, from top to bottom, 1, 5, 10, and 40 cm. These solid lines are shifted vertically one by one.

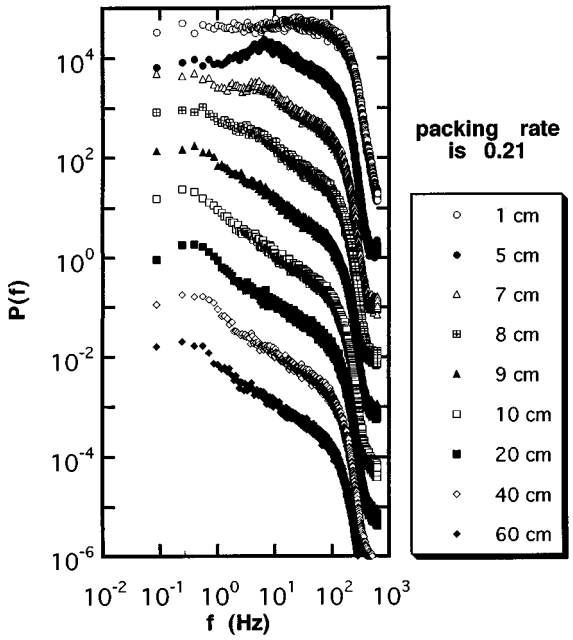

FIG. 8. Power spectra of the density fluctuation as functions of the frequency f for $p=0.21$ at the various measuring positions x. Here we used lead spheres 1.7 mm in diameter, a glass pipe 9.0 mm in inner diameter, and water as the liquid. From top to bottom, the measuring position x is $x=1$, 5, 7, 8, 9, 10, 20, 40, and 60 cm. The vertical scale for each spectrum is shifted appropriately. The spectrum at each x was obtained by averaging over ten trials.

f at various x for $p=0.21$. Just below the hopper ($x=1$ cm), metallic spheres fall freely from the hopper, the time evolution of the light intensity is random, as seen in Fig. 7, and its power spectrum takes a white-noise form, as seen in Fig. 8. As metallic spheres fall down through a pipe, the density fluctuation grows. First, the power spectrum at the high-frequency range increases, as shown by the power spectrum at $x=5$ in Fig. 8. Next, that of the low-frequency range increases. We found that at $x=10$ cm slugs begin to appear and the power spectrum obeys a beautiful power law $P(f)\sim 1/f^{\alpha}$ with $\alpha=0.83\pm 0.01$ over a frequency range 0.5–50 Hz. The time evolution of the transmitted light intensity at $x=10$ cm in Fig. 7 looks scale invariant and resembles that of the intermediate packing rate ($p\sim 0.18$) in Fig. 3. That is, the power-law power spectrum is observed only at the slugging transition point from the free-fall region towards the slugging region, and controlling physical parameters for each case were the packing rate p in Fig. 5 and the distance x from the hopper in Fig. 8, respectively. As we increase the value of x further, we obtain stable density waves (slugs) and power spectra no longer obey power laws. (See the power spectrum at $x=20$ cm in Fig. 8.) We also note, from power spectra at $x=20$, 40, and 60 cm in Fig. 8, that, after metallic spheres fall 20 cm down from the hopper, the granular flow takes the stationary structure that no longer depend on the value of x. The first 20 cm from the hopper is a transient region for the formation of the density fluctuation, and in that transient region we can observe the self-organization of the power spectrum.

Next, in Fig. 9 we present our results for the intermediate packing rate $p=0.18$ as functions of f at various x. As metallic spheres fall from the hopper down through the pipe, functional forms of power spectra evolve from the white-noise form at $x=1$ cm to the power-law form $P(f)\sim 1/f^{\alpha}$ at $x=20$ cm with $\alpha=0.80\pm 0.01$ over a frequency range

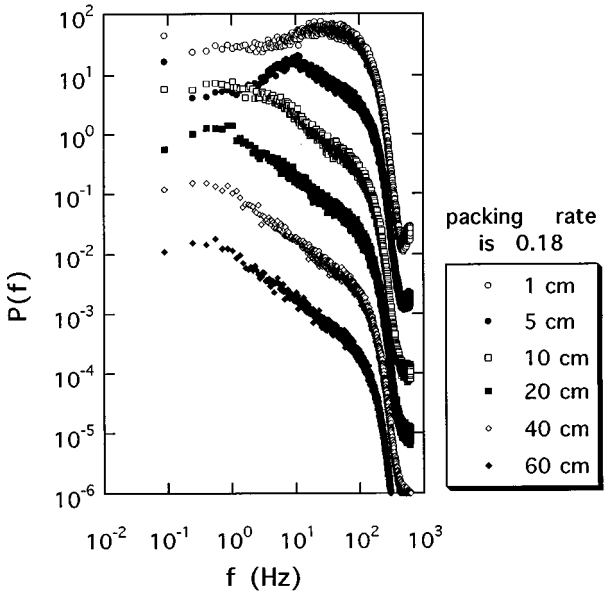

FIG. 9. Power spectra of the density fluctuation as functions of the frequency f for $p=0.18$ at the various measuring positions x. Here we used lead spheres 1.7 mm in diameter, a glass pipe 9.0 mm in inner diameter, and water as the liquid. From top to bottom, the measuring position x is $x=1$, 5, 10, 20, 40, and 60 cm. The vertical scale for each spectrum is shifted appropriately. The spectrum at each x was obtained by averaging over ten trials.

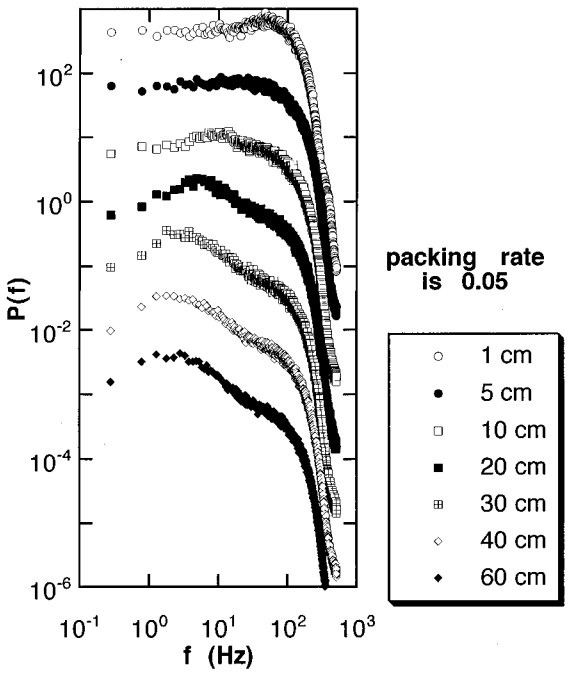

FIG. 10. Power spectra of the density fluctuation as functions of the frequency f for $p=0.05$ at the various measuring positions x. Here we used lead spheres 1.7 mm in diameter, a glass pipe 9.0 mm in inner diameter, and water as the liquid. From top to bottom, the measuring position x is $x=1$, 5, 10, 20, 30, 40, and 60 cm. The vertical scale for each spectrum is shifted appropriately. The spectrum at each x was obtained by averaging over ten trials.

0.5–50 Hz. On the other hand, even though we increase the value of x further, power spectra retain the same power-law form. That is, power spectra at $x=40$ and 60 cm also obey the same power law, $P(f)\sim 1/f^{\alpha}$ with $\alpha=0.81\pm 0.01$ over a frequency range 0.5–50 Hz. This means that the power spectrum acquires a final stationary structure after metallic spheres fall 20 cm down from the hopper, which shows that the slugging transition occurs for the intermediate packing rate.

Finally, Fig. 10 shows power spectra in the low-packing-rate free-fall region. Here the value of p is 0.05. Since the packing rate of metallic spheres is relatively low, the density fluctuation cannot grow enough. Therefore, even far from the hopper, power spectra do not show definite tendencies and are white-noise-like in the low-frequency range.

To summarize this section, we present a simple schematic illustration in Fig. 11. In our experiments, metallic spheres fall almost freely from the hopper and thus the power spectrum at the hopper exit has the white-noise form at any packing rate. As metallic spheres fall down through a pipe, the nonuniform granular flow is self-organized. First, the high-frequency part of the power spectrum increases, which suggests the growth of the microscopic density fluctuation of falling metallic spheres. In the low-packing-rate free-fall region, this is the final stationary structure, as shown in Fig. 11(a). When the value of the packing rate becomes larger, the low-frequency part of the power spectrum starts to increase at the next stage. This indicates the formation of a macroscopic density fluctuation that causes slugging. At the

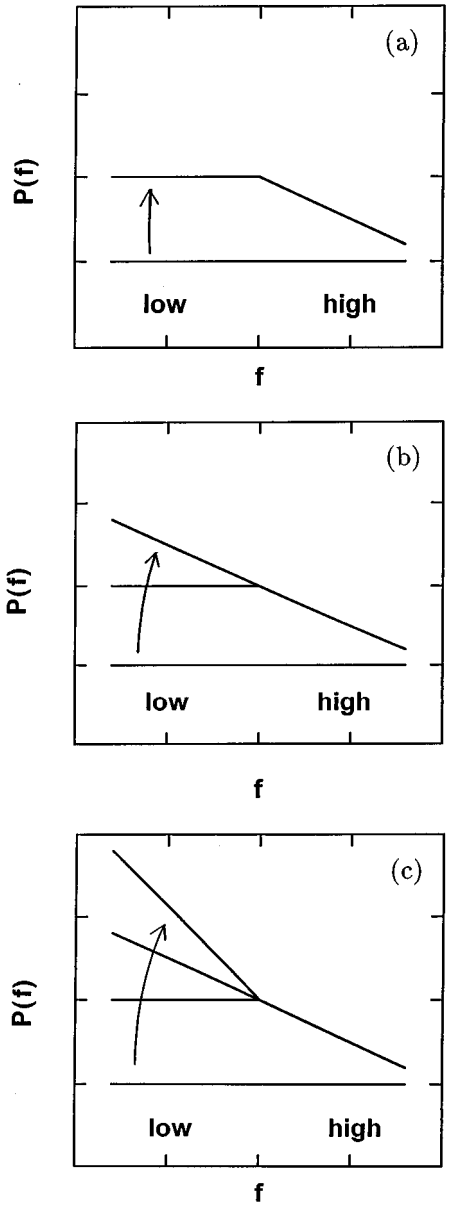

FIG. 11. Schematic illustration of the self-organization of power spectra $P(f)$ with various packing rate region: (a) in the low-packing-rate free-fall region, (b) at the intermediate packing rate (i.e., the slugging transition point), and (c) in the high-packing-rate slugging region.

slugging transition point ($p\sim 0.18$) the low-frequency part and the high-frequency part of the final power spectrum obey the same power law $P(f)\sim 1/f^{\alpha}$ [see Fig. 11(b)]. If we increase the packing rate further, many stable slugs are produced at the final stage, the amplitude of the low-frequency part of the power spectrum increases too much, and the final power spectrum no longer obeys the single power law, as illustrated in Fig. 11(c).

V. EXPERIMENTS USING SILICONE OIL

In this section we report on our experiments in which we use silicone oil as the liquid. Here we use stainless-steel spheres as metallic spheres because lead induces the gelation

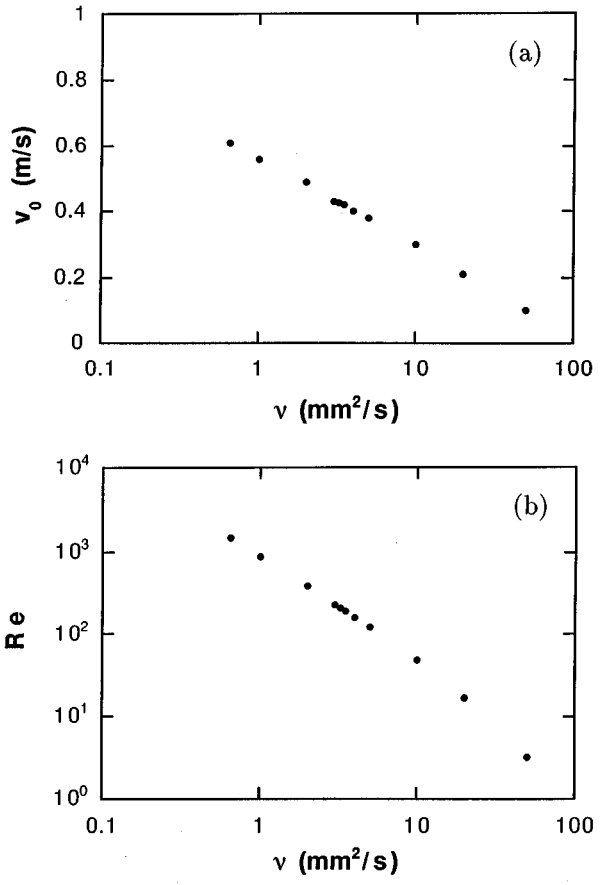

FIG. 12. Free-fall velocity v_0 of a single stainless-steel sphere 1.6 mm in diameter, presented as a function of the logarithm of the kinematic viscosity ν of the silicone oil. (b) Reynolds number Re of a freely falling single stainless-steel sphere 1.6 mm in diameter, presented as a function of the kinematic viscosity ν of the silicone oil.

of silicone oil. Of course, in water, the granular flows of lead spheres and of stainless-steel spheres are almost the same, except for the difference in the values of the free-fall velocity v_0 of a single metallic sphere due to the differences in both the size of a sphere and the density of the bulk of spheres. The density of the bulk of lead spheres is 11.34 g/cm^3 and that of stainless-steel spheres is 7.83 g/cm^3.

In our experiments the kinematic viscosity ν of silicone oil is varied as $\nu=0.65$, 1.00, 2.00, 3.00, 3.24, 3.50, 4.00, 5.00, 10.0, 20.0, and 50.0 mm^2/s. Accordingly, the experimental value of the mean free-fall velocity v_0 of a single stainless-steel sphere 1.6 mm in diameter varies as $v_0=0.61$, 0.56, 0.49, 0.43, 0.43, 0.42, 0.40, 0.38, 0.30, 0.21, and 0.10 m/s. Figure 12(a) shows the value of v_0 as a function of the logarithm of the kinematic viscosity ν of silicone oil. We also present, in Fig. 12(b), the value of Reynolds number, Re, of a freely falling single metallic sphere as a function of ν.

We use a glass pipe 7 mm in inner diameter and 1500 mm in length, but we do not use the additional hopper in this section. As we change the kinematic viscosity of the silicone oil, the input rate of metallic spheres from the hopper varies even though we are not using the additional hopper. As seen in Figs. 12(a) and 13, the kinematic viscosity of the liquid

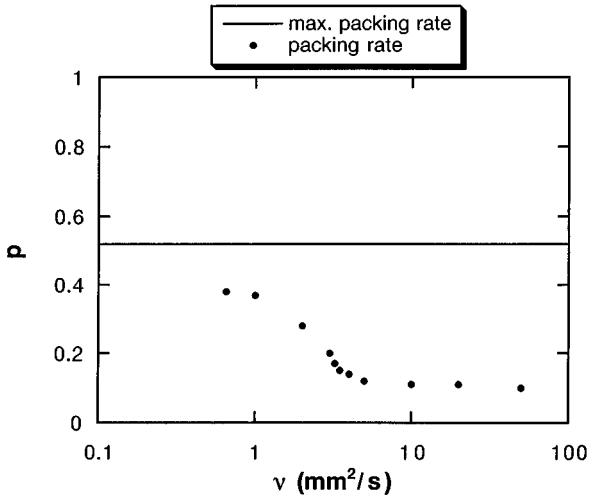

FIG. 13. Packing rate p, denoted by solid circles, as a function of the logarithm of the kinematic viscosity ν of the silicone oil. Here we used stainless-steel spheres 1.6 mm in diameter, a glass pipe 7.0 mm in inner diameter, and the silicone oil as the liquid. The horizontal solid guide line represents the maximum packing rate $p_m=0.52$ for this case.

inside the pipe changes not only the free-fall velocity of a single metallic sphere through a pipe but also the packing rate of metallic spheres inside the pipe. To investigate the general feature of the granular flow through a pipe, we

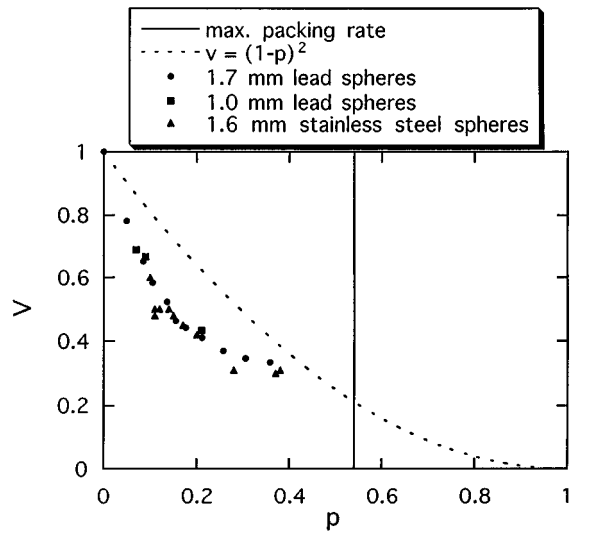

FIG. 14. Normalized relative velocity between the falling metallic spheres and the ascending fluid V plotted as a function of the packing rate p. Solid circles denoted the data of the case of the lead spheres 1.7 mm in diameter, a glass pipe 9.0 mm in inner diameter, and water as the liquid. The vertical solid guide line represents the maximum packing rate $p_m=0.54$ for this case. Solid squares denote the data of the case of the lead spheres 1.0 mm in diameter, a glass pipe 7.0 mm in inner diameter, and water as the liquid. Solid triangles represent the data of the case of the stainless-steel spheres 1.6 mm in diameter, a glass pipe 7.0 mm in inner diameter, and silicone oil as the liquid. The maximum packing rates p_m for the latter two cases are 0.56 and 0.52, respectively, but we omit them in the figure. The dotted guide line denotes V of the gravity-dominated flow in an infinite system and is given by $V=(1-p)^2$.

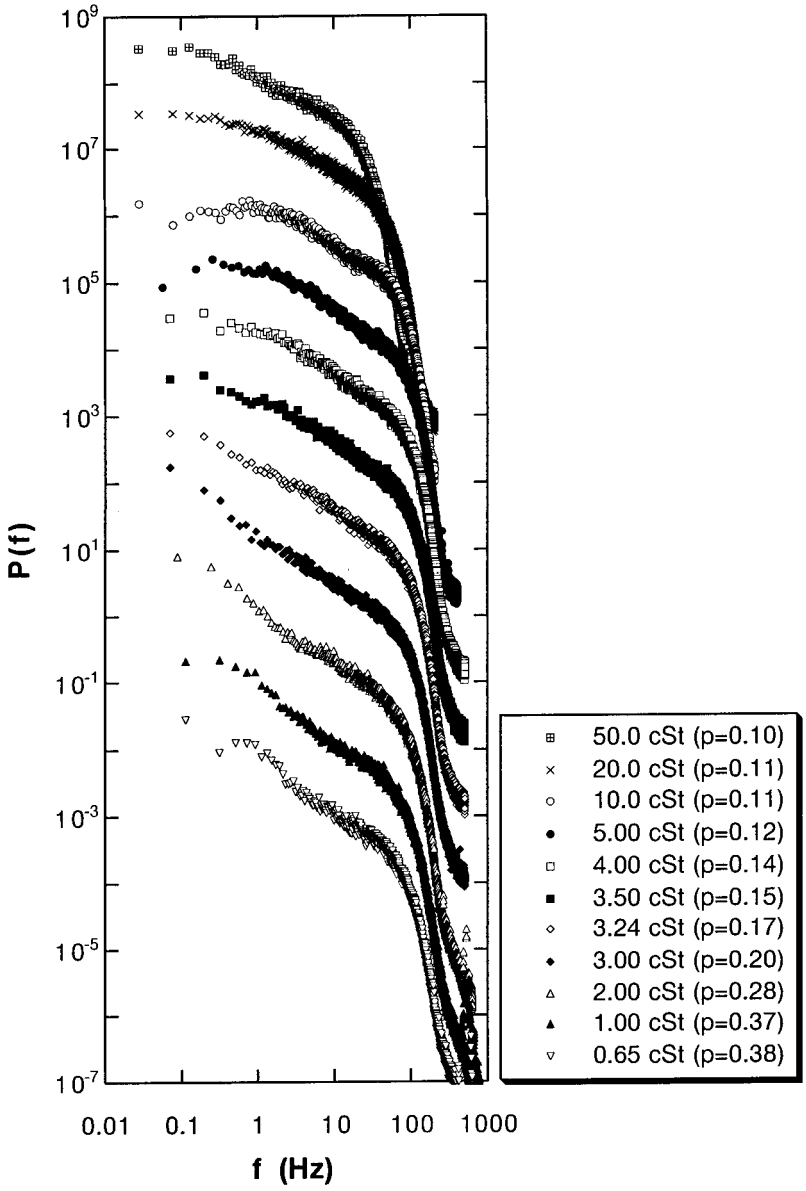

FIG. 15. Power spectra of the density fluctuation are plotted as functions of the frequency f at $x=1000$ mm for the various kinematic viscosities ν of silicone oil and at the same time for the various packing rates p. Here we used stainless-steel spheres 1.6 mm in diameter, a glass pipe 7.0 mm in inner diameter, and silicone oil as the liquid. From top to bottom, the kinematic viscosity ν of silicone oil is $\nu=50.0$, 20,0, 10.0, 5.00, 4.00, 3.50, 3.24, 3.00, 2.00, 1.00, and 0.65 cSt (here cSt = mm^2/s). At the same time, the packing rate p is, from top to bottom, $p=0.10$, 0.11, 0.11, 0.12, 0.14, 0.15, 0.17, 0.20, 0.28, 0.37, and 0.38. The vertical scale for each spectrum is shifted appropriately. The spectrum at each p was obtained by averaging over ten trials.

should perform experiments in which we control both the free-fall velocity v_0 of a single sphere and the packing rate p of metallic spheres independently. These experiments are still under investigation.

In Fig. 14 we present the normalized relative velocity V [defined by Eq. (3)] as a function of the packing rate p of metallic spheres inside the pipe. First, solid circles represent V for the case of lead spheres in Sec. III. The data are the same as those shown already in Fig. 4.

Also, we present, in Fig. 14, V of lead spheres 1.0 mm in diameter in water and denote them by solid squares. The free-fall velocity v_0 of a single lead sphere 1.0 mm in diameter is $v_0=0.45$ m/s in water. Here the inner diameter of the glass pipe is 7.0 mm. The maximum packing rate is $p_m=0.56$. The packing rate without the additional hopper is $p=0.21$. By using the additional hopper, we can decrease the packing rate as $p=0.21$, 0.09, and 0.07.

Solid triangles in Fig. 14 represent V of stainless-steel spheres 1.6 mm in diameter in silicone oil with various viscosities. The inner diameter is 7.0 mm and $p_m=0.52$. The relation between the kinematic viscosity ν of the silicone oil and the value of the packing rate p has already been presented in Fig. 13. Even though we are using water and silicone oil with various viscosities, all the data in Fig. 14 can be fitted by the same line when they are plotted as a normalized relative velocity V.

Next, Fig. 15 shows power spectra as the functions of the frequency f for the various kinematic viscosities ν of the silicone oil and at the same time for the various packing rates p. The length of the glass pipe is 1500 mm and the measuring position is $x=1000$ mm this case. Comparing Fig. 15 with Fig. 5, we find a similar systematic change in the functional forms of power spectra. As for the power spectra in the high-packing-rate slugging region ($p>0.18$), the slope of the low-frequency part ($f<3$ Hz) is larger than that of the high-frequency part ($f>3$ Hz) and thus power spectra do not obey the single power law in both figures. In the low-packing-rate free-fall region ($p<0.18$), but when $\nu<20$ mm^2/s, the low-frequency part cannot grow enough and thus power spectra do not obey the power law in both Figs. 5 and 15. Only at the

intermediate packing rate $p \sim 0.18$ is the power-law power spectrum obtained. That is, these power spectra are represented mainly as functions of the packing rate p, except for the high-kinematic-viscosity region ($\nu > 20\ \mathrm{mm}^2/\mathrm{s}$).

The high kinematic viscosity of liquid prevents the growth of the density fluctuation of granular materials and thus granular materials fall homogeneously through a pipe. When we compare the power spectrum for $\nu = 10\ \mathrm{mm}^2/\mathrm{s}$ with that for $\nu = 20\ \mathrm{mm}^2/\mathrm{s}$ in Fig. 15, we notice that the functional forms of these power spectra are different even though the packing rate p takes the same value $p = 0.11$. The situation with $\nu = 20\ \mathrm{mm}^2/\mathrm{s}$ corresponds to the case where the mean Reynolds number of falling metallic spheres in the granular flow is 8. From these results, we can conclude that in the high-Reynolds-number condition (Re > 10) the granular flow through a pipe is described mainly by the packing rate of granular materials inside the pipe just like the jamming transition in traffic flows, while in the low-Reynolds-number condition (Re < 10) the dissipation due to the viscosity of liquid is not negligible and the granular flow cannot be described only by the packing rate p.

VI. SUMMARY

To investigate the granular flow through a pipe, we performed experiments in which we used smooth metallic spheres of almost equal sizes as granular materials and water and silicone oil as liquid filling the pipe. We systematically controlled two physical parameters: a packing rate of the metallic spheres inside the pipe and a kinematic viscosity of the liquid that fills the pipe.

First, we observed the slugging transition from the low-packing-rate region ($p < 0.18$), where most metallic spheres fall freely, to the high-packing-rate region ($p > 0.18$), where metallic spheres become slugged and fall in group very slowly. The FFT analysis showed that only at the slugging transition point ($p \sim 0.18$) the power spectrum of the density fluctuation of falling metallic spheres obeys the single power law $P(f) \sim 1/f^{\alpha}$ over a wide frequency range, where f is a frequency and α is a positive constant.

Second, we investigated the self-organizations of nonuniform granular flows as metallic spheres fall down from the hopper through a glass pipe. We found that the granular flow evolves from the white-noise flow at the hopper exit toward the nonuniform flow through the pipe and the final stationary structure of the nonuniform flow depends on the packing rate of metallic spheres inside the pipe.

Finally, we performed experiments using the silicone oil with various viscosities and found that in the high-Reynolds-number condition (Re > 10) the nonuniform granular flow through a pipe is described mainly by the packing rate p when all physical variables are rescaled by the free-fall velocity, while in the low-Reynolds-number condition (Re < 10) the high viscosity of liquid prevents the growth of the nonuniform granular flow.

ACKNOWLEDGMENTS

We would like to acknowledge Professor H. Hayakawa, Professor S. Sasa, Dr. Y-h. Taguchi, S. Horikawa, K. Ichiki, H. Itoh, N. Kuroiwa, Y. Matsuo, O. Moriyama, T. Nakayama, I. Ràfols, and Y. Shimada for valuable advice concerning our experiments. We also thank Professor M. Katori and Dr. Y. Nakahara for critical readings of our manuscript.

[1] H. M. Jaeger and S. R. Nagel, Science **255**, 1523 (1992).
[2] *Granular Matter*, edited by A. Mehta (Springer, New York, 1994).
[3] H. M. Jaeger, S. R. Nagel, and R. P. Behringer, Phys. Today **49** (4), 32 (1996).
[4] G. W. Baxter, R. P. Behringer, T. Fagert, and G. A. Johnson, Phys. Rev. Lett. **62**, 2825 (1989).
[5] G. W. Baxter and R. P. Behringer, Phys. Rev. A **42**, 1017 (1990).
[6] G. H. Ristow and H. J. Herrmann, Phys. Rev. E **50**, R5 (1994).
[7] T. Pöschel, J. Phys. (France) I **4**, 499 (1994).
[8] S. Horikawa, A. Nakahara, T. Nakayama, and M. Matsushita, J. Phys. Soc. Jpn. **64**, 1870 (1995).
[9] T. Raafat, J. P. Hulin, and H. J. Herrmann, Phys. Rev. E **53**, 4345 (1996).
[10] J. Lee and M. Leibig, J. Phys. (France) I **4**, 507 (1994).
[11] J. Lee, Phys. Rev. E **49**, 281 (1994).
[12] G. Peng and H. J. Herrmann, Phys. Rev. E **49**, R1796 (1994).
[13] G. Peng and H. J. Herrmann, Phys. Rev. E **51**, 1745 (1995).
[14] D. F. Othmer, *Fluidization* (Reinhold, New York, 1956).
[15] *Fluidization*, edited by J. F. Davidson, R. Glift, and D. Harrison (Academic, London, 1985).
[16] K. Ichiki and H. Hayakawa, Phys. Rev. E **52**, 658 (1995).
[17] K. Nagel and M. Schreckenberg, J. Phys. (France) I **2**, 2221 (1992).
[18] O. Biham, A. A. Middleton, and D. Levine, Phys. Rev. A **46**, R6124 (1992).
[19] K. Nagel and H. J. Herrmann, Physica A **199**, 254 (1993).
[20] M. Takayasu and H. Takayasu, Fractals **1**, 860 (1993).
[21] B. S. Kerner and P. Konhäuser, Phys. Rev. E **48**, R2335 (1993).
[22] J. A. Cuesta, F. C. Martínez, J. M. Molera, and A. Sánchez, Phys. Rev. E **48**, R4175 (1993).
[23] F. C. Martínez, J. A. Cuesta, J. M. Molera, and R. Brito, Phys. Rev. E **51**, R835 (1995).
[24] K. Nagel, Phys. Rev. E **53**, 4655 (1996).
[25] T. Musha and H. Higuchi, Jpn. J. Appl. Phys. **15**, 1271 (1976).
[26] T. Nagatani, J. Phys. Soc. Jpn. **62**, 2533 (1993).
[27] K. Nagel, Int. J. Mod. Phys. C **5**, 567 (1994).
[28] K. Nagel and M. Paczuski, Phys. Rev. E **51**, 2909 (1995).
[29] X. Zhang and G. Hu, Phys. Rev. E **52**, 4664 (1995).
[30] M. Y. Choi and H. Y. Lee, Phys. Rev. E **52**, 5979 (1995).
[31] G. B. Wallis, *One-Dimensional Two-Phase Flow* (McGraw-Hill, New York, 1969).
[32] P. Bak, C. Tang, and K. Wiesenfeld, Phys. Rev. Lett. **59**, 381 (1987).